DOI: 10.1002/ejic.201100152

Synthesis, Swelling, and Exfoliation of Microporous Lamellar Titanosilicate AM-4

Clara Casado,[a] Diego Ambroj,[a] Álvaro Mayoral,[b] Eugenio Vispe,[c] Carlos Téllez,[a] and Joaquín Coronas*[a]

Keywords: Intercalations / Layered compounds / Adsorption / Organic–inorganic hybrid composites / Zeolite analogues

AM-4 is a layered porous titanosilicate built from TiO_6 and SiO_4 polyhedra. An improved synthesis of AM-4 crystals enabling control of particle size by secondary growth and reducing synthesis time is presented. A new material, UZAR-S2, has been obtained by exfoliation of the smaller AM-4. The exfoliation consists of proton exchange with acetic acid, intercalation with nonylamine, and final activation by washing with HCl/water/ethanol. Besides XRD, TEM, N_2 adsorption, FTIR, and UV/Vis characterization highlighting the delaminated character of UZAR-S2, CO_2 adsorption was also measured.

Introduction

Microporous titanosilicates belong to the octahedral–pentahedral–tetrahedral frameworks (OPT) family of mixed siliceous materials.[1] They have potential applications in fields typically associated with zeolites (adsorption, catalysis, membranes, and ion exchange) and also in the areas of optics, batteries, magnetism, and sensors.[2] One important advantage of these materials is their preparation under hydrothermal conditions at temperatures from 150 to 230 °C without using costly organic structure-directing agents. The synthesis of zeolites may result in layered structures whose delamination can give fine particles with high aspect ratios and the theoretical thickness of a single layer, and as such, delaminated zeolites have been prepared from the delamination process of lamellar precursors such as MCM-22P,[3] AMH-3,[4] PREFER,[5] and Nu-6(1).[6,7] These particles have potential in a number of applications such as ion exchange and catalysis,[3,8] enhancing the permselectivity of polymer–zeolite nanocomposite membranes,[9] the immobilization of enzymes,[10] and producing polymer-layered silicate nanocomposites with improved tensile properties.[11] Layered sodium titanium silicates have recently been reported,[12] and the delamination of Ti-MWW, which is postsynthesized from the highly deboronated MWW zeolite,[13] succeeded. AM-4 is a layered titanosilicate, which was first reported in 1997[14] and its structure was established by Dadachov et al.[15] It is a monoclinic layered solid, with the molecular formula $Na_3(Na,H)Ti_2O_2(Si_2O_6)_2 \cdot 2H_2O$, built from TiO_6 octahedra and SiO_4 tetrahedra forming five-tier $Si_{Td}/Ti_{Oh}/Si_{Td}/Ti_{Oh}/Si_{Td}$ (Td: tetrahedral; Oh: octahedral) sandwiches (Figure S1). It also contains intra- (in small cages within the layers) and interlayer Na^+ cations, and water molecules.

The swelling and exfoliation of this material has not been reported to date. This work presents the synthesis and characterization of a new delaminated titanosilicate obtained from the exfoliation of AM-4, achieved by a procedure analogous to that developed in our laboratory for the delamination of the microporous titanosilicate JDF-L1.

Results and Discussion

Tuning the preparation conditions can control the particle size of zeolitic materials. From our previous experience with JDF-L1,[16] it was expected that the exchange and swelling capability would be enhanced with small crystals. Therefore, synthesis time, seeding, and the Ti source were explored in order to optimize the preparation of AM-4 crystals (Table 1). Two anatase precursors were used with different particle sizes, Ti1 (100–300 nm) and Ti2 (< 25 nm). The smaller Ti source, Ti2, was mainly used in this work, because it gave rise to a decrease in the size of the sheet-like crystals obtained (A and B in Table 1).

The use of seeding with preprepared AM-4 crystals (B) enabled the synthesis time to be reduced from 96 h to 6 h, without affecting the single particle growth habit and crystallinity of AM-4 (Figures 1 and 2). The seeding also con-

[a] Chemical and Environmental Engineering Department and Nanoscience Institute of Aragón, Universidad de Zaragoza, María de Luna 3, 50018 Zaragoza, Spain
Fax: +34-976-76-1871
E-mail: coronas@unizar.es
[b] Laboratorio de Microscopía Avanzada, Nanoscience Institute of Aragón, Universidad de Zaragoza, Mariano Esquillor s/n, 50018 Zaragoza, Spain
[c] Organic Chemistry Department and Instituto Universitario de Catálisis Homogénea, Universidad de Zaragoza, Pedro Cerbuna 12, 50009 Zaragoza, Spain

Supporting information for this article is available on the WWW under http://dx.doi.org/10.1002/ejic.201100152.

Table 1. Synthetic conditions of the AM-4 crystals at 230 °C.

ID	Ti source	Seeding	Time [h]	Size[a] [μm]
A	Ti1	–	96	*L*: 6.9 ± 0.8 *T*: 0.55 ± 0.13
B	Ti2	–	96	*L*: 3.9 ± 0.5 *T*: 0.28 ± 0.07
C	Ti2	B	24	*L*: 2.7 ± 0.3 *T*: 0.15 ± 0.03
D	Ti2	B	12	*L*: 1.3 ± 0.1 *T*: 0.06 ± 0.02
E	Ti2	B	6	*L*: 1.2 ± 0.2 *T*: 0.05 ± 0.02

[a] *L*: crystal length, *T*: crystal thickness (as observed by SEM on more than 30 particles of each compound).

tributed to an additional decrease in the dimensions of the plate-like crystals from 0.55 ± 0.13 × 6.9 ± 0.8 (Figure 1a, sample A in Table 1) to 0.05 ± 0.02 × 1.2 ± 0.2 μm (Figure 1d, sample E in Table 1) without varying the morphology of the layers. No other phases were observed by XRD for the synthesis conditions presented (Figure 2).

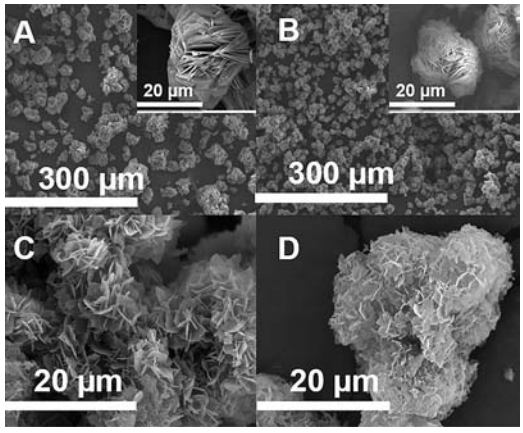

Figure 1. SEM micrograph of AM-4 aggregates: images A–D correspond to samples A, B, C, and E in Table 1.

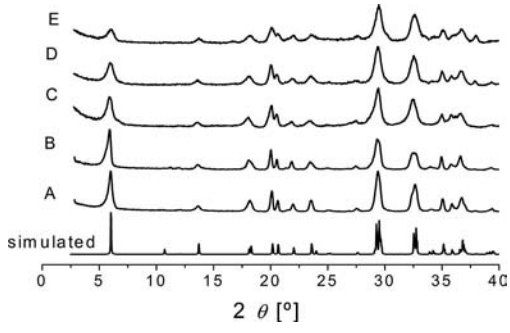

Figure 2. XRD patterns of AM-4 crystals prepared under the conditions listed in Table 1 (A–E correspond to samples A–E). The simulated pattern was obtained from atomic position data from Dadachov et al.[15] by using Powder Cell 2.4 software.[17]

Sample E was chosen to study the swelling of AM-4. To favor the intercalation of nonylamine molecules, proton exchange was carried out with acetic acid. A typical swelling procedure is as follows: a nonylamine aqueous solution (0.23 M) was stirred gently at 50 °C. After 10 min of reaction with the proton exchange agent solution, the nonylamine solution was added. The pH was then increased to 9, and the intercalation reaction proceeded at 60 °C for 12 h. The solid was washed five times by centrifugation (10000 rpm) and dried at 100 °C for 8 h. Figure S2 in the Supporting Information shows a thermogravimetric analysis (TGA) diagram of the swollen material compared with that of as-made AM-4. The delamination of AM-4, which gives rise to the formation of UZAR-S2, was complete when the amine molecules were removed by chemical extraction with HCl/H_2O/ethanol solution.

Under the optimum swelling conditions using acetic acid, the amount of amine intercalated was calculated by TGA as ca. 14.3 wt.-%, associated with the weight loss observed by TGA in the range 200–650 °C (Figure S2).[18] This means that approximately one amine molecule for each four exchangeable cation positions was intercalated, i.e. one amine molecule per AM-4 formula unit. It is worth mentioning that there are three different cationic sites (Na1, Na2, and Na3) with an Na1/Na2/Na3 = 2:1:1 relationship, according to the multiplicity of the cations reported by Dadachov et al.[15] The Na1 site is placed in the intralayer space, inaccessible to the protonated amine. Na2 and Na3 are found in gallery interlayer positions, i.e. half of the interlayer exchanging sites would be occupied by amine molecules. See Figure S1 and Table S1 in the Supporting Information for further details of these sites. Figure 3 reveals a peak for swollen AM-4 at $2\theta = 2.8°$ indexed to (002). This peak allows the estimation of a layer spacing of 31.0 ± 0.3 Å. This is comparable to that observed in the swelling of the layered titanosilicate JDF-L1 with a basal spacing of 29.6 ± 1.4 Å, and is consistent with a bilayer surfactant configuration,[19] as the nonylamine molecular length is about 14 Å. The spacing between the layers is corroborated by TEM.

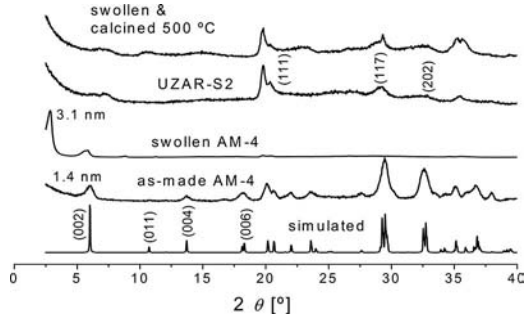

Figure 3. XRD patterns of AM-4 and its derivatives. Note that in the delaminated material the visible reflections are related to (*hkl*) planes with *h* and/or $k \neq 0$.

To gain an insight into the exfoliation process, the swollen and exfoliated materials were embedded in polysulfone (Figure 4, inset) to make a polymer–silicate composite,[7] which was cut with an ultramicrotome and observed by TEM. From over ten images, thicknesses were measured on 70 particles for each of the swollen and exfoliated materials. The normalized cumulative number of par-

ticles is presented in Figure 4 as a function of the particle thickness. From this representation, at an $N/N_T = 0.5$ ratio (N and N_T being the cumulative number of particles up to a given thickness and the total number of particles, respectively), an average particle thickness of 13.1 nm was obtained. From the structural data presented in Figure S1 in the Supporting Information and XRD patterns (Figure 2), the thickness of a single layer is 1.46 nm, thus, an average particle contains about nine layers, each consisting of a five-tier sandwich of $Si_{Td}/Ti_{Oh}/Si_{Td}/Ti_{Oh}/Si_{Td}$.[15] It is worth noting that the maximum particle thickness is 60 nm, which should correspond to that of a nonexfoliated particle. The swollen and exfoliated materials have almost the same cumulative distribution indicating that exfoliation mainly occurs during the swelling stage.

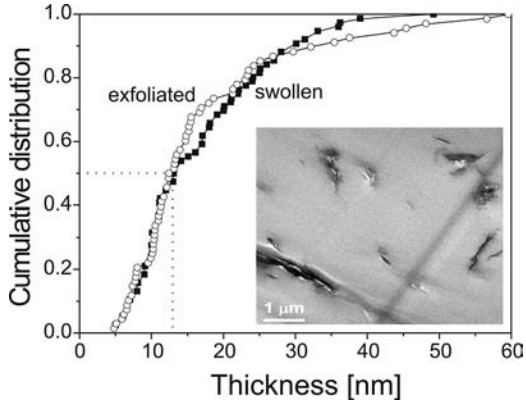

Figure 4. Normalized cumulative number of particles (N/N_T) as a function of particle thickness, for swollen and exfoliated material embedded in polysulfone. Inset: TEM image of swollen AM-4 embedded in polysulfone.

Elemental analysis was carried out by X-ray fluorescence (XRF) on Ti, Si, and Na, showing agreement with the theoretical values (Table 2). The Na/Ti ratio decreased upon swelling with nonylamine and further extraction in acid, corroborating the hypothesis of Na^+ exchange by protons. The Si/Ti ratio does not seem to decrease as much as it did for JDF-L1,[19] where the theoretical Si/Ti ratio of the layered precursor material is double that of AM-4.

Table 2. Atomic ratios obtained by XRF analysis.

Sample	Si/Ti	Na/Ti
Theoretical	2	1.5
AM-4 (E in Table 1)	1.5 ± 0.0	1.7 ± 0.0
Swollen AM-4	1.3 ± 0.0	0.66 ± 0.0
Delaminated AM-4 (UZAR-S2)	1.2 ± 0.0	0.13 ± 0.0

Electron microscopy analysis of UZAR-S2 showed a morphology very similar to that of the parent material AM-4, with thin particles deposited on top of each other. Figure 5 shows a typical image of the sheets obtained for the material after exfoliation. The electron diffraction (ED) pattern shown in the inset was indexed by assuming an *A*2/*a* (no. 15) space group. Two interlayer distances (Figure 5b) were measured by HRTEM for the exfoliated material: $d_1 \approx 1.3 \pm 0.1$ nm, which corresponds to the (002) plane in the parent solid, and $d_2 \approx 2.5 \pm 0.2$ nm. The distance d_2 is almost double d_1, which is in agreement with the XRD pattern observed for the swollen material prior to amine extraction. It is therefore clear that delamination is only partially achieved, and there are nonexfoliated particles present in the final product.

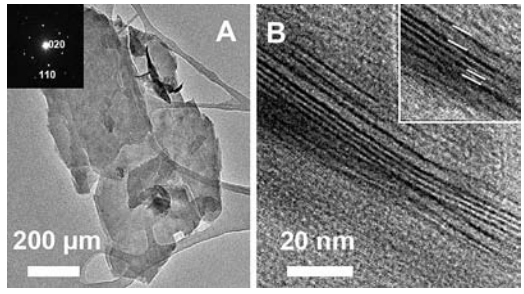

Figure 5. (A) TEM micrograph of a particle of UZAR-S2 oriented in the [001] direction. The ED pattern shown in the inset was indexed by assuming *A*2/*a* symmetry.[9] (B) TEM image of the product layers; a closer view is shown in the inset together with the interlayer distances.

According to the XRD data (Figure 3), there is no difference between the calcined and acid-extracted material. Nevertheless, the textural properties of AM-4 and UZAR-S2 are very different (Figure S3). AM-4 scarcely adsorbs N_2, and this is reflected by a BET specific surface area of only 2.4 ± 0.2 and 5.5 ± 0.0 m^2/g for the unseeded titanosilicate solid (samples A and B in Table 1, respectively). This is consistent with the only value of BET surface area found in literature of 7 m^2/g.[20] The seeded material obtained after 6 h of hydrothermal synthesis (sample E) has a BET surface area of 13.0 ± 0.1 m^2/g. Activation of UZAR-S2 was carried out by HCl extraction. An up-to-date maximum BET surface area of 122 ± 1 m^2/g was attained, if sonication steps are included before the chemical extraction, whereas without the sonication step, the BET surface area does not exceed 90 m^2/g. This suggests that even though exfoliation did not occur during extraction (Figure 4), sonication increased the amine extraction yield. The BET specific surface area is about ten times larger for UZAR-S2 than for its precursor, AM-4. Calcination at 400 °C was also performed on one of the swollen samples, obtaining a BET specific surface area of 83.3 ± 0.5 m^2/g. However, further calcination at 500 °C reduces the BET specific surface area to 61.6 ± 0.2 m^2/g. Similar behavior was observed for UZAR-S1,[19] in good agreement with the lower than expected thermal stability of titanosilicates in comparison with the typical high Si/Al ratio lamellar zeolites exfoliated in previous work.[3,6]

FTIR and ^{29}Si NMR investigations were conducted in order to corroborate the atomic arrangements in the AM-4 titanosilicate and modified materials, as a means to explain the structural differences that occur during exfoliation.

The FTIR absorption spectra are shown in Figure 6. The broad band present at 3600–3100 cm^{-1} is due to hydroxy groups that may come from either adsorbed water or silanol groups.[21] That the samples contain some water is con-

firmed by the band at 1640 cm^{-1}, which is assigned to adsorbed water.[22] The group of signals in the range 1250–900 cm^{-1}, attributed to siloxane bridges, show a structure similar to that of crystalline layered silicates except for the presence of a band at 950 cm^{-1} that is attributed to Si–O–Ti linkages.[23] The morphology of these bands changes as the material is swollen and delamination takes place. This process dramatically changes the shape of this region; the structure visible in the as-made AM-4 becomes blurred as it swells, and the intensity of the bands at 1060–1090 cm^{-1} increases as the material is extracted, showing that the distribution of the Si–O–Si linkages changes during this process. These bands are similar to those found in noncrystalline silica, which are mainly formed by highly crosslinked Q^4 sites.[24] This observation points to a partial condensation of the layered structure. In addition, it is worth mentioning the peaks at ca. 2900 cm^{-1}, corresponding to nonylamine molecules, which are still noticeable after the extraction step in UZAR-S2. From the difference in the TGA of calcined and extracted swollen materials (not shown), it is observed that about 5.2 wt.-% nonylamine is still present in the structure after acid extraction. Further extractions were not carried out to prevent loss of the very fine material.

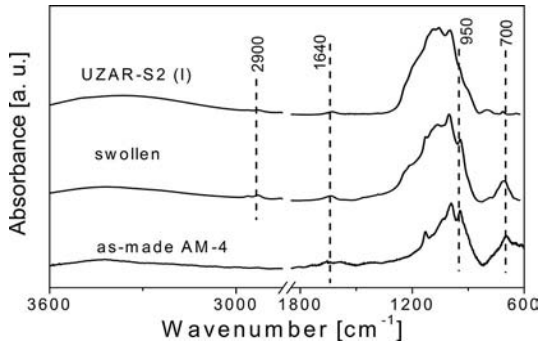

Figure 6. FTIR absorption spectra of AM-4 (E in Table 1) and derivatives.

Besides the changes observed in the Si–O–Si bridges, the strong decrease in intensity of the band at 950 cm^{-1}, showing that the Ti–O–Si linkages are broken during the extraction process, agrees with the titanium and silicon loss observed by XRF (see Table 2) and with the delamination process itself.[13] Despite the modification of the siloxane bridges, the band at ca. 1000 cm^{-1}, attributed to terminal siloxane Si–O with a nonbridging oxygen atom characteristic of Q^3 sites,[23] is present in the final extracted material, indicating that UZAR-S2, after the whole process, retains part of the original structure of AM-4, as has already been mentioned when discussing XRD and TEM results.

Further confirmation of the structural changes is observed from the disappearance of the band at ca. 700 cm^{-1}, which is attributed to Si–O asymmetric stretching in the internal tetrahedra of intralayer four-membered rings.[25] This band is present in both AM-4 and the swollen AM-4 samples but disappears in the delaminated samples, pointing to changes in the intralayer structure that may be due to silanol condensation.

As presented in Figure 7, the AM-4 structure displays two different Si sites with the same Si and Ti coordination [Si(2Si,1Ti)] but different distributions of exchangeable Na^+ cations. One of the sites is in the layer (Figure 7a) and the other is connected to the gallery space (Figure 7b). As can be observed in these two local environments, the Na^+ cations may have different accessibility, and an easier exchange can be assumed for those in the gallery (responsible for the intercalation properties of AM-4) than for those in the intralayer space. It has been noted that the distribution and nature of exchangeable cations in titanium–niobium silicates with nenadkevichite structure have a strong influence on the ^{29}Si chemical shift.[26] With this in mind, NMR spectroscopy is discussed in the following paragraph.

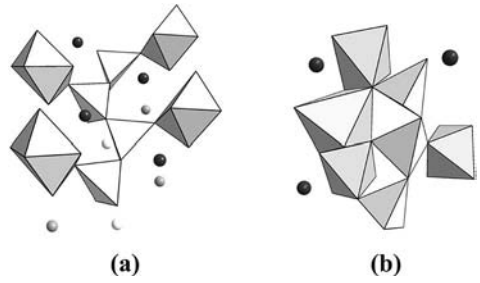

Figure 7. Schematic representation (by using DIAMOND 3.2) of the Si sites present in AM-4 structure: (a) interlayer or gallery Si1 and (b) intralayer Si2. White = Si, grey = Ti, black = Na1, intralayer cations, light grey and white = Na2 and Na3, gallery exchangeable cations.

In its ^{29}Si magic angle spinning (MAS) NMR spectrum, AM-4 displays a strong peak, as observed in Figure 8 at δ = –92.5 ppm, related to Si(2Si,1Ti), followed by two faint peaks, as reported by Lin et al.[14] These two peaks appear at δ = –94.9 and –106.0 ppm in both the as-made and swollen AM-4 materials. They are also attributed to Si(2Si,1Ti), with differences in the compensating cations due to washing, protonation, amine intercalation, and chemical extraction. Apart from this slight increase and the shift of the peaks corresponding to Si in the galleries to lower δ values, the swollen AM-4 has the same resonance (as well as both having the same FTIR signal at 700 cm^{-1}) indicating that the layered Si and Ti coordination is maintained. After delamination (sample UZAR-S2 in Figure 8), the spectrum can be deconvoluted into five main peaks at δ = –92.5, –99.1, –102.8, –110.4, and –117.8 ppm. The peak at δ = –92.5 ppm coincides with that of as-made AM-4, and is attributed to Si(2Si,1Ti), confirming partial delamination in agreement with the ca. 13 nm average particle thickness deduced from Figure 4. Layered silicates have been reported to lose their connectivity upon swelling and exfoliation,[9] but this band at higher resonance assigned here to the intralayer Si connections is still present in the exfoliated material. This would indicate that the Si and Ti coordination in the delaminated particles is maintained but also that a small fraction (Table S1) of the AM-4 precursor remains unconverted, as has already been pointed out in the discussion of the XRD, TEM, and FTIR results. The peaks at δ = –99.1 and –102.8 ppm are also attributed to an Si(2Si,1Ti) envi-

ronment but surrounded mainly by protons instead of Na^+ cations. This is attributed to the final proton exchange process (see Table 2, where the Na/Ti ratio is seen to have been reduced from 1.74 in as-made AM-4 to 0.13 in UZAR-S2). The peaks at δ = –110.4 and –117.8 ppm are assigned to Si(3Si,0Ti) and Si(4Si,0Ti) sites, respectively. This is a result of the leaching of Ti during the amine extraction in HCl/H_2O/ethanol,[13] leading to an increased Si(4Si,0Ti) contribution associated to the condensation of tetrahedral silica in those particles where delamination did not succeed completely.[4] This condensation can be linked to the disappearance of the FTIR band at 700 cm^{-1}. Attributions and connectivities are collected in Table S1.

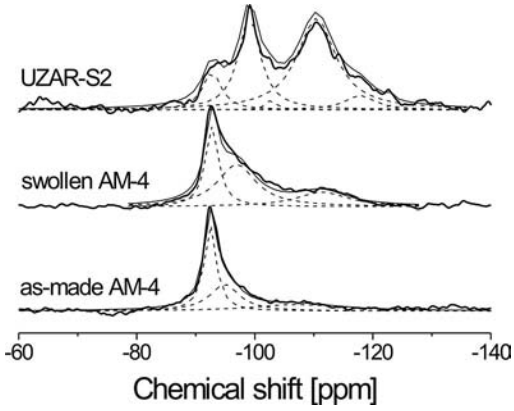

Figure 8. ^{29}Si MAS NMR spectra of AM-4 (E in Table 1) and derived materials.

After swelling with nonylamine, the ^{29}Si MAS NMR evolution suggests that exfoliation has already started. The exfoliation and the band at lower displacement increases, which will have been generated from the exchange of Na^+ by protons as observed for nenadkevichite and ETS-4,[27] in agreement with other observations on AM-4 material.[28] This effect could also be attributed to the breaking of X–O–X bonds (X = Si and Ti), which is consistent with the fine, high length/width ratio particles observed by TEM.[19]

Completing the spectroscopic analysis, Figure 9 shows the diffuse-reflectance ultraviolet/visible (DR-UV) absorption spectra of the samples. The spectra do not show any bands above 300 nm, which rules out the presence of anatase or rutile phases.[29] The maxima of the broad ligand-to-metal-charge-transfer (LMCT) bands are located above 230 nm. This is related to the octahedral nature of the Ti sites,[30] which are distorted by the effect of neighboring ligands such as H_2O, SiO, and SiOH. The as-made AM-4 shows the broadest band with its maximum at ca. 258 nm and a shoulder at about 290 nm, which can be assigned to framework Ti–O–Ti chains reported in other titanosilicates such as ETS-4.[31] After swelling, the LMCT band keeps its shape although slightly narrowed, possibly indicating that the intralayer framework of the Ti–O–Ti chains remains after the exchange of interlayer Na^+ ions. Finally, after delamination, the shape of the LMCT band changes dramatically, with its maximum shifted to 240 nm and the presence of a shoulder at ca. 260 nm. The main band is compatible with the formation of Si(3Si,0Ti) species,[32] whereas the shoulder suggests the presence of some Ti–O–Ti species still present after exfoliation.

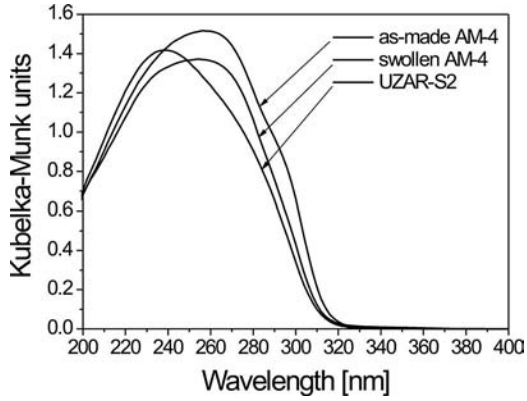

Figure 9. DR-UV absorption of AM-4 (E in Table 1) and derived materials.

These results provide evidence that UZAR-S2 is a delaminated material obtained from the layered titanosilicate AM-4. As a preliminary attempt at exploiting the features of this novel material, CO_2 adsorption experiments were conducted at 298 K, and the results are given in Figure 10. The CO_2 adsorption capacity of UZAR-S2 is about five times higher than that of original AM-4, because the delaminated product has a higher specific surface area available than the layered precursor. Although the maximum capacity of UZAR-S2 is lower than the value of 2 mmol CO_2/g obtained for the microporous titanosilicate ETS-10,[33] which possesses an important internal surface area as well as a larger pore volume, the maximum capacity is in the same range as that of Ti-umbite (about 0.2 mmol CO_2/g).[34]

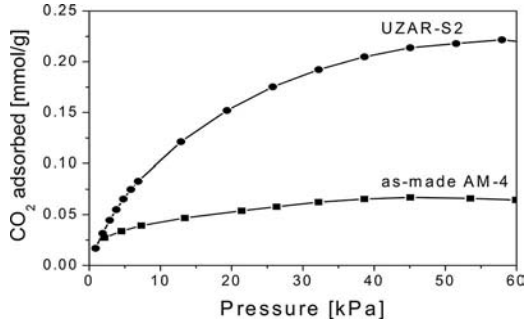

Figure 10. CO_2 adsorption of seeded AM-4 (E in Table 1) and its delaminated product UZAR-S2.

Conclusions

The seeding procedure can help reduce the synthesis time of AM-4 without compromising the purity of the crystalline phase. The size reduction observed is thought to assist in the swelling and delamination of the material. XRD, TEM, FTIR, NMR, and DR-UV characterizations suggest an intercalation process that affects the material as a whole but preserves the layer structure. The partial delamination (as

the average particle thickness is about 13 nm and the NMR spectrum still shows features from the as-made material) carried out here gives rise to UZAR-S2, which preserves the structural features of AM-4, obtaining a final product with more active sites available for adsorption demonstrated by N_2 and CO_2 adsorption experiments.

Experimental Section

Lamellar microporous titanosilicate AM-4 was synthesized at 230 °C by a seeded secondary-growth procedure. A typical seeded synthesis (to produce about 2.5 g of solid) was as follows: To an Na_2SiO_3 solution (10.050 g, 27 wt.-% SiO_2, 8 wt.-% Na_2O, Merck) was added NaOH (1.420 g), distilled water (6.550 g), and a TiO_2 source (0.770 g, 99.8 wt-%, Aldrich). This gel, with a molar composition of 4.2 SiO_2/TiO_2/2.9 Na_2O/68 H_2O and a pH of 12.1, was stirred at room temperature for 1 h. Preprepared ground, unseeded AM-4 (prepared with the same gel composition at 230 °C for 96 h) was then added in a 0.45 wt.-% ratio to the gel as seeds. The gel was introduced into a Teflon-lined autoclave and heated in an oven at 230 °C for 6–24 h. The material obtained was swollen by intercalation of nonylamine (97 wt.-%, Alfa Aesar) after proton exchange in the presence of diluted acetic acid or HCl aqueous solutions. In a typical procedure, 0.23 M acetic acid (glacial, Alfa Aesar) was prepared in deionized water at 60 °C with stirring and a pH of 3–4 was measured. Proton exchange occurred upon addition of AM-4 (220 mg) over 10 min before adding an aqueous nonylamine solution (0.23 M, 1.806 g amine in 55 mL deionized water). The pH then increased abruptly to a value of about 9 which was maintained with stirring at 60 °C for 12 h. The resulting product was centrifuged at 10000 rpm for 15 min, and the solid was recovered in acetone and dried at 100 °C for 8 h.

To remove the amine, the solid collected (200 mg) was mixed with a HCl/H_2O/EtOH solution (50 mL, 5 HCl/17 H_2O/870 EtOH, molar composition) and heated at 55 °C for 8 h. Prior dispersion of the swollen material in ethanol, before addition of HCl, improved the exfoliation yield. The slurry obtained was washed five times with deionized water and centrifuged. The solid recovered (UZAR-S2) was dried at 100 °C for 20 h.

The materials were characterized by X-ray diffraction using a D-Max Rigaku X-ray diffractometer (Cu-K_α radiation, λ = 1.5418 Å, step size = 0.03°, 2θ = 2.5–40°). After degassing at 200 °C for 10 h, a Micromeritics Tristar 3000 was used to analyze the BET specific surface area. CO_2 sorption isotherms were measured for AM-4 and UZAR-S2 at room temperature with a Micromeritics ASAP 2020 setup, after outgassing at 200 °C for 10 h. SEM (JEOL 6400) images were obtained from Au-coated specimens, at 20 kV. XRF was measured with a ThermoElectron, ARL series, model ADVANT'XP equipped with an X-ray tube with Be front window and Rh anode. Samples were measured as pellets under vacuum. UNIQUANT software (ThermoScientific) was used to obtain a semiquantitative analysis of the elements. TEM analysis was performed with a FEI TECNAI F30 at 300 kV. The samples were prepared by repeated dispersion in ethanol and acetone before pouring onto the carbon grid. FTIR spectra were recorded with a Nicolet Avatar 360 FTIR spectrometer from wafers diluted with KBr treated under vacuum ($< 10^{-5}$ Torr) at 140 °C for 2 h in a cell equipped with NaCl windows. ^{29}Si solid-state MAS NMR spectra were recorded with a Bruker AV400 WB spectrometer operating at a resonance frequency of 79.49 MHz with a 4 mm probe. The measurements were carried out with a contact time of 3.5 ms, a pulse width of 4 μs, a recycle delay of 5 s, and a spinning rate of 10 kHz. DR-UV spectra (190–400 nm) were recorded with a Jasco V-670 spectrometer, equipped with a Harrick Praying Mantis accessory, from pure samples previously dried overnight at 140 °C under vacuum. The scattering intensity was measured with respect to a $BaSO_4$ standard.

Supporting Information (see footnote on the first page of this article): Figure S1: views of the AM-4 structure; Figure S2: TGA of swollen AM-4, using different protonation agents; Figure S3: N_2 adsorption/desorption isotherms of AM-4 and UZAR-S2; Table S1: Fractions of the NMR for AM-4 and the products from swelling and delamination.

Acknowledgments

Financing from the Spanish Ministry of Science and Innovation (MAT2007-61028, CIT-420000-2009-32) and the Government of Aragón (PI035/09) is gratefully acknowledged. C. C. also thanks the Ministry for the "Juan de la Cierva" programme.

[1] J. Rocha, Z. Lin, *Rev. Mineral. Geochem.* **2005**, *57*, 173–201.
[2] J. Rocha, M. W. Anderson, *Eur. J. Inorg. Chem.* **2000**, 801–818.
[3] A. Corma, V. Fornes, S. B. Pergher, T. L. M. Maesen, J. G. Buglass, *Nature* **1998**, *396*, 353–356.
[4] S. Choi, J. Coronas, E. Jordan, W. Oh, S. Nair, F. Okamoto, D. F. Shantz, M. Tsapatsis, *Angew. Chem. Int. Ed.* **2008**, *47*, 552–555.
[5] A. Corma, U. Díaz, M. E. Domine, V. Fornes, *J. Am. Chem. Soc.* **2000**, *122*, 2804–2809.
[6] A. Corma, V. Fornes, U. Díaz, *Chem. Commun.* **2001**, 2642–2643.
[7] P. Gorgojo, A. Galve, S. Uriel, C. Téllez, J. Coronas, *Micropor. Mesopor. Mater.* **2011**, *142*, 122–129.
[8] G. Centi and S. Perathoner, *Microporous Mesoporous Mater.* **2008**, *107*, 3–15.
[9] H.-K. Jeong, W. Krych, H. Ramanan, S. Nair, E. Marand, M. Tsapatsis, *Chem. Mater.* **2004**, *16*, 3838–3845; S. Choi, J. Coronas, J. A. Sheffel, E. Jordan, W. Oh, S. Nair, D. F. Shantz, M. Tsapatsis, *Microporous Mesoporous Mater.* **2008**, *115*, 75–84.
[10] A. Corma, F. Vornés, J. L. Jordá, F. Rey, R. Fernandez-Lafuente, J. M. Guisan, B. Mateo, *Chem. Commun.* **2001**, 419–420.
[11] Z. Wang, T. J. Pinnavaia, *Chem. Mater.* **1998**, *10*, 1820–1826.
[12] A. Clearfield, A. I. Bortun, L. N. Bortun, R. A. Cahill, *Solvent Extr. Ion Exch.* **1997**, *15*, 285–304.
[13] P. Wu, D. Nuntasri, J. F. Ruan, Y. M. Liu, M. Y. He, W. B. Fan, O. Terasaki, T. Tatsumi, *J. Phys. Chem. B* **2004**, *108*, 19126–19131.
[14] Z. Lin, J. Rocha, P. Brandao, A. Ferreira, A. P. Esculcas, J. D. P. d. Jesus, A. Philippou, M. W. Anderson, *J. Phys. Chem. B* **1997**, *101*, 7114–7120.
[15] M. S. Dadachov, J. Rocha, A. Ferreira, Z. Lin, M. W. Anderson, *Chem. Commun.* **1997**, 2371–2372.
[16] C. Rubio, C. Casado, S. Uriel, C. Téllez, J. Coronas, *Mater. Lett.* **2009**, *63*, 113–115.
[17] W. Kraus, G. Nolze, *J. Appl. Crystallogr.* **1996**, *29*, 301–303.
[18] C. B. A. Lima, C. Airoldi, *Solid State Sci.* **2002**, *4*, 1321–1329.
[19] C. Rubio, C. Casado, P. Gorgojo, F. Etayo, S. Uriel, C. Téllez, J. Coronas, *Eur. J. Inorg. Chem.* **2010**, 159–163.
[20] S. Lima, A. S. Dias, Z. Lin, P. Brandao, P. Ferreira, M. Pillinger, J. Rocha, V. Calvino-Casilda, A. A. Valente, *Appl. Catal. A* **2008**, *339*, 21–27.
[21] J. Bu, H.-K. Rhee, *Catal. Lett.* **2000**, *65*, 141–145.
[22] M. D. Alba, A. I. Becerro, J. Klinowski, *J. Chem. Soc., Faraday Trans.* **1996**, *92*, 289–292.
[23] J.-A. Kim, J.-K. Suh, S.-Y. Jeong, J.-M. Lee, S.-K. Ryu, *J. Ind. Eng. Chem.* **2000**, *6*, 219–225.

[24] W. Lutz, D. Täschner, R. Kurzhals, D. Heidemann, C. Hübert, *Z. Anorg. Allg. Chem.* **2009**, *635*, 2191–2196.
[25] S. Nair, Z. Chowdhuri, I. Peral, D. A. Neumann, L. C. Dickinson, G. Tompsett, H. K. Jeong, M. Tsapatsis, *Phys. Rev. B* **2005**, *71*, 104301–104308.
[26] J. Rocha, P. Brandao, Z. Lin, A. P. Esculcas, A. Ferreira, M. W. Anderson, *J. Phys. Chem.* **1996**, *100*, 14978–14983.
[27] J. Rocha, P. Brandao, Z. Lin, A. Kharlamov, M. W. Anderson, *Chem. Commun.* **1996**, 669–670.
[28] V. Kostov-Kytin, B. Mihailova, Y. Kalvachev, M. Tarassov, *Microporous Mesoporous Mater.* **2005**, *86*, 223–230.
[29] F. Geobaldo, S. Bordiga, A. Zechina, E. Giamello, G. Leofanti, G. Petrini, *Catal. Lett.* **1992**, *16*, 109–115.
[30] O. A. Kholdeeva, N. N. Trukhan, *Russ. Chem. Rev.* **2006**, *75*, 411–432.
[31] B. Yilmaz, J. Warzywoda, A. Sacco Jr., *Nanotechnology* **2006**, *17*, 4092–4099.
[32] J. M. Fraile, J. I. García, J. A. Mayoral, E. Vispe, *J. Catal.* **2005**, *233*, 90–99.
[33] A. Anson, C. C. H. Lin, S. M. Kuznicki, J. A. Sawada, *Chem. Eng. Sci.* **2009**, *64*, 3683–3687.
[34] V. Sebastián, J. Bosque, I. Kumakiri, R. Bredesen, A. Ansón, J. A. Maciá-Agulló, Á. Linares-Solano, C. Téllez, J. Coronas, *Microporous Mesoporous Mater.* **2011**, DOI: 10.1016/j.micromeso.2011.01.010.

Received: February 15, 2011
Published Online: March 25, 2011

